 doi:10.20944/preprints201902.0124.v1

Ligand-Protein Interactions: A Hybrid *ab initio*/Molecular Mechanics Computational Study

Yornei R. Perez[a], ***Dinais Alvarez***[a], and ***Aldo F. Combariza***[*,a]

[a]*in silico Molecular Modeling and Computational Simulation Research Group, Department of Biology and Chemistry, Faculty of Education and Sciences, University of Sucre, Colombia*

[*]aldo.combariza@unisucre.edu.co

Preprints (www.preprints.org) | NOT PEER-REVIEWED | Posted: 13 February 2019 doi:10.20944/preprints201902.0124.v1

Abstract

The enzymes Cyclooxygenase (COX) or prostaglandin-endoperoxide synthase (PTGS) are important in the synthesis of prostaglandins, which are the main mediating chemi- cals at inflammatory processes. The body produces two highly homologous COX isoforms, cyclooxygenase-1 (COX-1) and cyclooxygenase-2 (COX-2). COX-1 is involved in the pro- duction of prostaglandins which take part in physiological processes such as: protection of the gastric epithelium, maintenance of renal flow, platelet aggregation, neutrophil mi- gration and also expressed in the vascular endothelium; Meanwhile COX-2 is inducible by proinflammatory stimuli. To counteract the symptoms of inflammation, nowadays is very frequent the use of nonsteroidal antiinflammatory drugs (NSAIDs); These drugs in addi- tion to other benefits, can also cause side effects on people's health (cardiovascular and respiratory problems, in the nervous system, among others). Due to the above, it is neces- sary to accelerate the investigations that allow to know in more detail the mechanisms of action that involve the use of natural plant products as pharmacological agents. In the pre- sent research, computational techniques are used, especially those based on the Molecular Docking Method to know the protein-ligand interaction in systems of biological interest. It was possible to determine the structure-activity relationship in inflammatory processes involving the participation of a number of secondary plant metabolites such as luteolin, galangin, kaempferol, apigenin, morine and quercetin on the inactivation of the enzyme cyclooxygenase (COX-1 and COX -2). In the COX-1 / ligand coupling it was found that apigenin was the ligand which showed the lowest coupling energy with a value of -8.88, whereas quercetin showed the highest value (-6.65); for the coupling COX-2 / ligand the apigenin also showed the lowest energy value (-8.93), while kaempferol showed the highest value (-7.51). This shows that apigenin is the ligand with the best stability within the active site of both enzymes. On the other hand, quercetin showed the highest relative selectivity with a protein-ligand selectivity index (PLSI) of 1.17, while kaempferol showed an PLSI of 0.91. Taking into account the parameters of stability and selectivity we can say that of all the ligands used, quercetin would be the ideal to block COX-2.

Keywords enzymes Cyclooxygenase, ligand, metabolites, antiinflammatory, Molecular Docking.

Preprints (www.preprints.org) | NOT PEER-REVIEWED | Posted: 13 February 2019 doi:10.20944/preprints201902.0124.v1

Introduction

The awe-inspiring development of computational performance in the last decades has open the door to a new way of doing science, which is usually referred as computational experimentation or *in silico* experimentation.[1–3] In general, an *in silico* experiment begins by modeling a real system using solid theoretical physical principles, followed by the simulation of the system through computer programmed mathematical algorithms.[3–5]

In this work, we use a hybrid *ab initio*/mechano-statistical technique to study the features of biological macromolecules, proteins, and their interactions with low molecular weight chemical species, called ligands. These protein-ligand biological systems, are a paradigmatic example of the structure-activity principle.[5,6] We use here the Molecular Docking (MDock) technique, which allows us to predict the most appropriate conformation of a molecule (ligand) when it binds to another (protein) to form a stable complex.[6] In fact, the use of MDock its seen as a advantageous technique in the study of protein-ligand interactions within the field of drug discovery and development.[7–9]

In this case, we intend to understand the structure-activity relationship of the ligand-protein interactions from an atomistic point of view and, therefore, to attain relevant information to disclose the effect of a biological active molecule, or ligand, on a specific proteic target.[10] One relevant proteic target, very useful in the clinical research field, is the Prostaglandin−endoperoxide synthase (PTGS) or Cyclooxygenase (COX) enzyme.[11,12] The first isoform is constitutive, and executes indispensable functions in the organism, while the second isoform intervenes in inflammatory processes, becoming the target of study for the search of novel anti-inflammatory compounds.[13] Both, COX-1 and COX-2, have a high structural similarity, only differing by the relative position of three amino acids. This structural similarity brings about non-selectivity between COX-1 and COX-2, *e.g.*, non steroidal anti-inflammatory drugs (NSAIDs) are not selective for COX, which causes serious consequences in the organism.[13,14]

The lack of NSAIDs-COX selectivity, has fueled the search for new molecules or ligands. Sometimes these ligands are obtained from natural sources, that is, secondary metabolites from plants or animals, some of which are recognized to have a higher COX selectivity, helping to avoid or minimize the side effects produced by NSAIDs in the body.[15,16]

Within the secondary metabolites obtained from plants, we have a very wide group of chemicals

Preprints (www.preprints.org) | NOT PEER-REVIEWED | Posted: 13 February 2019 doi:10.20944/preprints201902.0124.v1

known as flavonoids, which include: flavones, flavonols, antocyanidins and isoflavonols.[17] These metabolites are recognized as anti-allergenic, anti-thrombotic, anti-oxidant and anti-inflammatory effects.[18] Some examples of vegetal species which are used to extract these compunds are: *Dioclea grandiflora, Sophora flavescens, Swinglea glutinosa* and *Muntingia calabura*.[15]

The aim of this work is to use tools of computational biochemistry to describe the structure-activity relationship between COX-ligand systems, which is of paramount importance in inflammatory inhibition, involving the action of secondary metabolites.

Methodology

COX structural characterization

COX-1

From the Protein Data Bank (PDB)[19], we have extracted 217 structures directly related with COX-1. These structures were discriminated according to the species from which they have been obtained, and are distributed as follows: *Homo sapiens* (51), *Bos taurus* (29), *Mus musculus* (25), *Ovis aries* (22), *Escherichia coli* (12), *Rattus norvegicus* (12), *Zea mays* (10), others species (53).[19] Currently, there is a record of 171 ligands that form complexes with COX-1, among which are flurbiprofen, arachidonic acid, ibuprofen, sodium ion and nitric acid.[19,20]

COX-2

For COX-2, we have found 220 structures from the PDB, which were extracted from species like: *Homo sapiens* (51), *Mus musculus* (43), *Bos taurus* (28), *Ovis aries* (21), *Escherichia coli* (12), *Rattus norvegicus* (12), *Saccharomyces cerevisiae* (8), others (42).[19] For this COX isoform, there are 178 ligands recognized, among which are the following: acetylsalicylic acid, flurbiprofen, urea, arachidonic acid and ibuprofen.[20]

For COX-1 we have used the model corresponding to *Ovis aries* (PDB ID: code 3N8Z) and for COX-2, the one for*Mus musculus* (PDB ID: code 1CX2) and the experimental method used to dilucidate the tertiary structures of COX's was ray's x crystallography.[21,23] These structures were selected because, according to Kurumbail *et al*, human COX-2 has a similarity of 87% with the murine enzyme, and the amino acid sequence that forms the active site is conserved between both species,

Preprints (www.preprints.org) | NOT PEER-REVIEWED | Posted: 13 February 2019 doi:10.20944/preprints201902.0124.v1

therefore, we expect that human COX-2, and mainly the active site, will behave similarly to murine enzyme.[23]

COX enzymes preparation and active sites identification.

COX enzymes belongs to the oxidoreductase protein family, and forms complexes with selective inhibitors such as SC-558.[23] pdb-files downloaded from the PDB-database, are provided as tetramer for COX-2 and as a dimer for COX-1.[21] On the other hand, PyMOL[26] was used to eliminate hemo groups, water molecules and ligands present in the structure of the enzyme.

Ligands characterization

The ChemSpider[27] database was used to retrieve the chemical species of interest.[28] These species are secondary metabolites coming from plants, belonging to the flavonoid family. We have selected the following metabolites as subjects of study:

- Apigenin (5,7-Dihydroxy-2-(4-hydroxyphenyl)-4H-chromen-4-one)[29]
- Luteolin (2-(3,4-Dihydroxyphenyl)-5,7-dihydroxy-4H-chromen-4-one)[30]
- Quercetin (2-(3,4-Dihydroxyphenyl)-3,5,7-trihydroxychromen-4-one)[31]
- Morin (2-(2,4-Dihydroxyphenyl)-3,5,7-trihydroxy-4H-chromen-4-one)[32]
- Galangin (3,5,7-Trihydroxy-2-phenyl-4H-chromen-4-one)[33]
- Kaempferol (3,5,7-Trihydroxy-2-(4-hydroxyphenyl)-4H-chromen-4-one)[34]

Geometry optimization

Geometry optimization is a molecular modeling technique that allows us to obtain the structural conformations of lowest energy of a molecule by determining the critical points of the potential energy function and the rotations of chemical bonds that form the molecule.[35,36] With this information we predict the tridimensional disposition of the atoms in a molecule creating a potential energy surface.[35–39]

MOPAC[40] was used to optimize the ligands chemical structures. MOPAC is a program based on the theoretical principles of quantum mechanics (QM), that is, the use of semi-empirical methods

Preprints (www.preprints.org) | NOT PEER-REVIEWED | Posted: 13 February 2019 doi:10.20944/preprints201902.0124.v1

to predict properties of chemical structures and model chemical reactions.[41] MNDO, MINDO/3, AM1 and PM3 were the Hamiltonians used to achieve molecular orbitals, heat of formation and its derivatives with respect to molecular geometry.[41–44] Followed by the calculation of properties like: vibration spectra, thermodynamic quantities and constant forces that corresponds to molecules, radicals, ions and polymers.[42,43] After the ligand optimization, we define parameters like the torsion center and the rotable bonds of the ligands.

Molecular Docking

Before the MDock process, we add the hydrogen bonds missing to COX structures. This step is carried out because the hydrogen atoms have a small nuclei and are very mobile, so they are not detected by the X rays in crystallographic process. AutoDock Vina (AUV)[45] was used to behave the MDock Process. AUV uses a Lamarckian Genetic Algorithm (LGA) and a free-energy Empirical Punctuation Function (EPF) that allows a faster search method and provides reproducible results in larger systems.[46–48] This software uses a semi-empiric force-field to evaluate the free-energy of conformations along the coupling simulations. At the same time, the force-field is parameterized using experimental information recover from numerous protein-inhibitor systems.[46]

We consider ten conformations for each protein-ligand interaction.

Selectivity index and stability index

We determine a index of selectivity and stability for each COX-ligand interaction. The stability index was determined by dividing each energetic value by the lowest energetic value. Whereas, the selectivity index was determined by dividing the binding energy of each ligand/COX-2 interaction between the binding energy of each ligand-COX-1 interaction, taking into account the correspondence between the ligands. Finally, the values obtained were normalized.

Results and Discussion

Molecular characterization of COX

The tertiary structures of COX are very similar, thus, they share the same folding units. Because of this, we use the COX-1 structure to characterize both enzymes. We can divide the tertiary structure

Preprints (www.preprints.org) | NOT PEER-REVIEWED | Posted: 13 February 2019 doi:10.20944/preprints201902.0124.v1

of COX-1 in three folding units, showed in Figure 1.

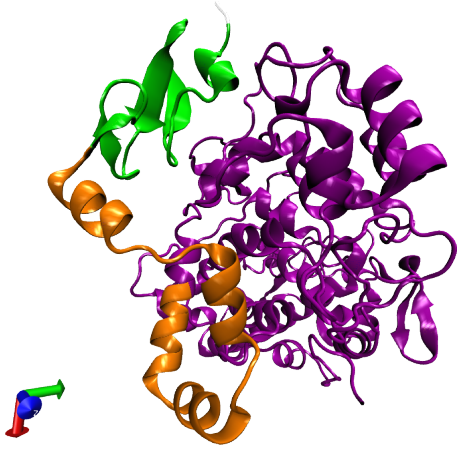

Figure 1: Folding units of COX-1. First unit is show in green, the second is show in orange and the third is show in violet.

The first folding unit is formed by residues 34-72 in positions amino-terminal and form a small compact domain binded by three disulfide bonds, as Figure 2A shows. The global conformation of this domain, including the disposition of the disulfide bonds, is very similar to the conformation of the epidermal growth factor and binds covalently to the principal chain of the enzyme by another disulfide bridge, that is, Cys-37-Cys-159. The second unit is formed by residues 73-116 and form a structure of alpha helix A, B, C and D that are located at one side of the first folding unit, as we illustrate in Figure 2B. These alpha helix are highly amphipathic and represents a structural motif for the insertion of enzyme to the lipid bilayer. And the last folding unit consist of a large catalytic globular domain formed by residues 117-587. This catalytic domain is a globular structure that contains the cyclooxygenase and peroxidase active sites. Both sites, peroxidase and cyclooxygenase, comprise two differents lobes in the polypeptidic chain although interlaced with each other. The largest lobe is made by a structure formed by seven alpha helices, whereas the smallest lobe of the catalytic domain is formed by six alpha helices. These alpha helices form a set, more or less parallel, with its axes (see Figure 2C).

Preprints (www.preprints.org) | NOT PEER-REVIEWED | Posted: 13 February 2019 doi:10.20944/preprints201902.0124.v1

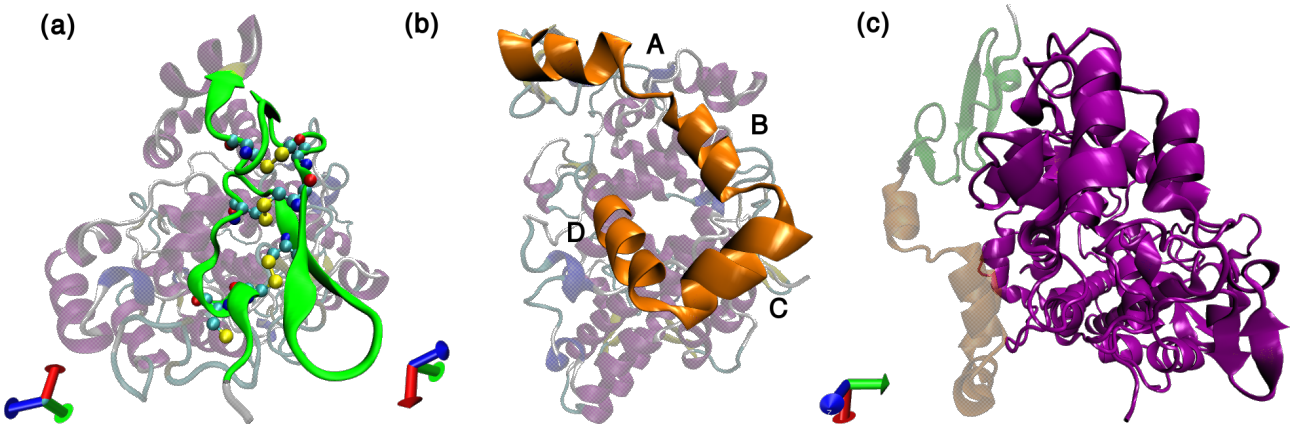

Figure 2: Folding units of COX-1. (a) first folding unit in green and the three disulfide bonds are shown in yellow; (b) in orange is show the second folding unit and the four alpha helices (A, B, C and D); (c) in violet, the third folding unit is represent by alpha helices and beta sheets.

Characterization of the secondary structures of COX

Table 1: COX-1 secondary structure characterization

Coil		3-10 Helix	Alpha helix	Beta sheet
32-34	324	35-38	74-81	46-50
39-41	354-362	281-283	86-93	54-58
63	370-377	363-366	97-105	64-65
70	391-394	388-390	107-121	71-72
73	403	498-500	139-143	130-131
82-85	411	538-540	174-182	149-150
94-96	418	547-550	196-207	245-248
106	428-429		238-244	251-252
129	431		296-319	255-257
135-138	433-439		325-353	260-262
148	459-462		379-385	395-397
154-155	471-477		404-407	400-402
167	483-484		412-417	
172-173	496-497		419-427	
188	501-502		445-458	
211	510-511		463-470	
236-237	517-518		478-482	
253-254	537		485-495	
263-264	546		503-509	
271-275	551-552		520-536	
280	562-563		553-561	
284	571		564-570	
286	576-580			
	582-584			

Preprints (www.preprints.org) | NOT PEER-REVIEWED | Posted: 13 February 2019 doi:10.20944/preprints201902.0124.v1

Table 2: COX-2 secondary structure characterization

Coil		3-10 Hélices	Hélices alfa	Láminas Beta
33	263-264	363-366	74-81	46-49
40	271-275	388-390	86-94	55-58
63	324	498-500	97-104	64-65
70	354-362	538-540	106-121	71-72
73	370-377		139-143	245-248
82-85	391		174-182	251-252
95-96	396		196-209	255-257
105	401		238-243	260-262
129-130	403		296-317	
138	418		325-353	
148	428-431		379-384	
154-155	437-439		404-407	
167	459-461		411-417	
172-173	471-477		419-427	
188	483-484		444-458	
195	501		463-470	
210-212	510-511		478-482	
236-237	561-563		485-495	
244	576-580		503-509	
253-254			520-533	
			553-560	
			564-571	

Topological and molecular characterization of the active sites of COX

The active sites of COX enzymes have a high similarity. Both active sites consist of a hydrophobic channel with an approximate extension of 25 Angstroms. This channel originates in the Membrane Binding Domain (MBD) and extends to the nucleus of the globular domain.[21–23] The amino acids covering the hydrophobic channel of COX active sites are: Leu117, Arg120, Val434 (COX-2), Ile434 (COX-1), Phe205, Phe209, Val344, Ile345, Tyr348, Val349, Leu352, Ser353, Tyr355, Leu359, Phe381, Leu384, Tyr385, Trp387, Phe518, Ile523 (COX-1), Val523 (COX-2), Gly526, Ala527, Ser530, His513 (COX-1), Arg513 (COX-2), Leu531, Gly533, Leu534 and these are shown in Figure 3. Only three of the channel residues are polar Arg120, Ser353 y Ser530.

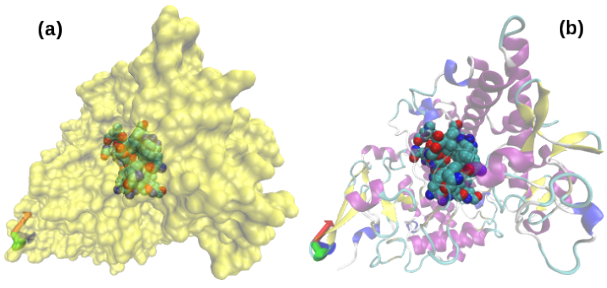

Figure 3: Amino acids of COX active site. (a) In the center of the figure are shown the amino acids that form the active site of the enzyme, highlighting the third folding unit.

Preprints (www.preprints.org) | NOT PEER-REVIEWED | Posted: 13 February 2019 doi:10.20944/preprints201902.0124.v1

The residue Ser530 is acetylated by aspirin, while the residue Arg120 binds to the carboxylate groups of the fatty acids and many NSAIDs.[49–52]

The size of the active site of COX-2 is approximately about 20% more large that the COX-1 enzyme. This difference in the active sites of COX is very important due to the variation of three residues at positions 434, 513 and 523 of both enzymes, as we show in Figure 4. The variation in the size of both active sites has been an important feature for the development of specific NSAIDs for COX-2.[53] Figure 5 shows, an superposition of the active sites of both enzymes with the residues that differentiate them, at the same point.

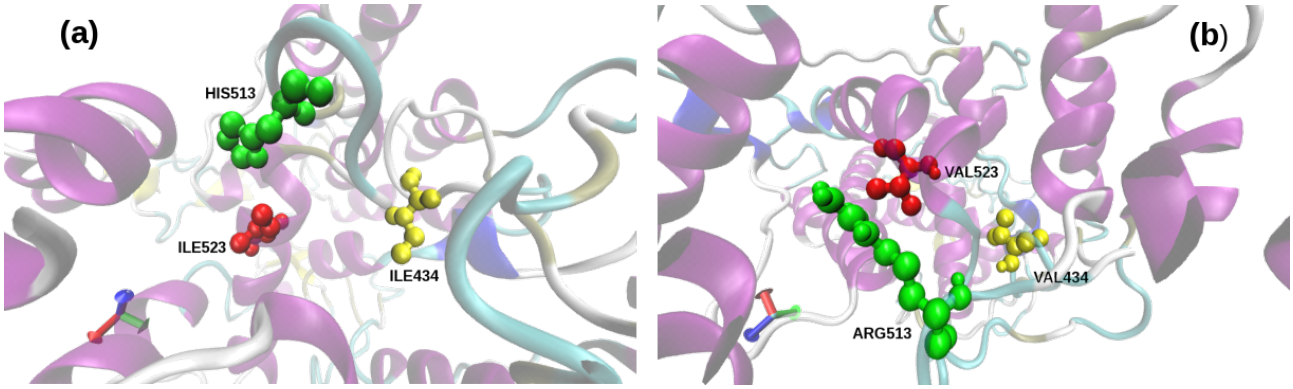

Figure 4: Amino acids that differentiate the active sites of COX. A. Amino acid Ile434 is highlighting in yellow, His513 in green and Ile523 in red to COX-1. B. Amino acids of COX-2 are highlighting as: Val434 in yellow, Arg513 in green and Val523.

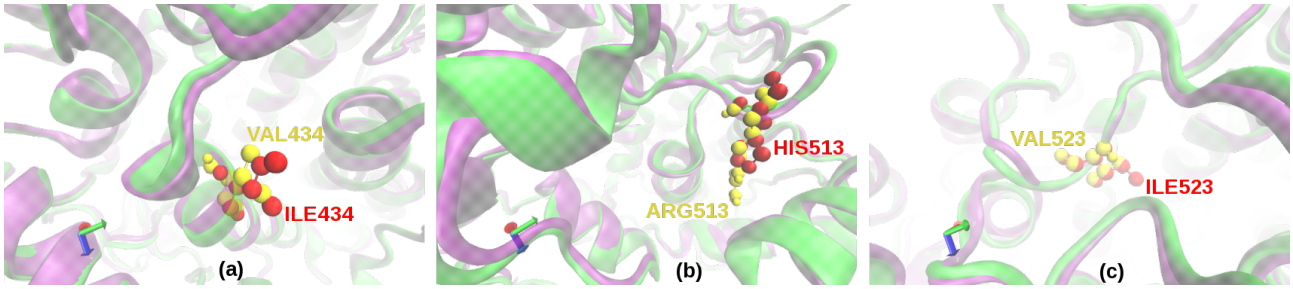

Figure 5: Superposition of COX active sites. COX-1: green, COX-2: violet. (a) isoleucin for COX-1 and valine for COX-2; (b) histidin for COX-1 and arginin for COX-2; (c) isoleucin for COX-1 and valin for COX-2.

Geometry optimization

Table 3 shows the values obtained from the calculation of minimization energies and the calculation of molecular orbitals HOMO and LUMO of each ligand. These values are ordered according to the HOMO energy from the best nucleophile to the best electrophile. The HOMO orbital is the last orbital that is doubly occupied and shows where the pair of electrons most susceptible to electrophilic

Preprints (www.preprints.org) | NOT PEER-REVIEWED | Posted: 13 February 2019 doi:10.20944/preprints201902.0124.v1

attacks is located. Taking into account the values shown in Table 1, we can see that, of all the ligands, galangin is the best nucleophile, while apigenin is the worst nucleophile.

Table 3: Minimization energy values and molecular orbitals HOMO and LUMO

Ligand	Galangin	Kaempferol	Quercetin	Morin	Luteolin	Apigenin
Total Energy	-3452.9	-3748.7	-4044.0	-4043.9	-3749.0	-3453.7
HOMO	-8.974	-9.075	-9.099	-9.147	-9.351	-9.458
LUMO	-0.755	-0.997	-1.084	-0.8	-1.18	-1.071

It should be noted that the calculations of the energies of the molecular orbitals HOMO and LUMO was made to know the distribution of the electrical charges along the molecule. Therefore, interactions with electrophilic groups are controlled by the HOMO orbital, while the nucleophilic attacks are controlled by the LUMO orbitals. Thus, Figure 6 allow us to observe, in a spatial way, the distribution of the charges and the regions of the molecule with high electron density, that is, regions susceptible to electrophilic and nucleophilic attacks. These areas also show the electrostatic potential of the molecules, the red color shows the negative part and the blue color shows the positive part. The green and yellow regions show the poorest electron zones.

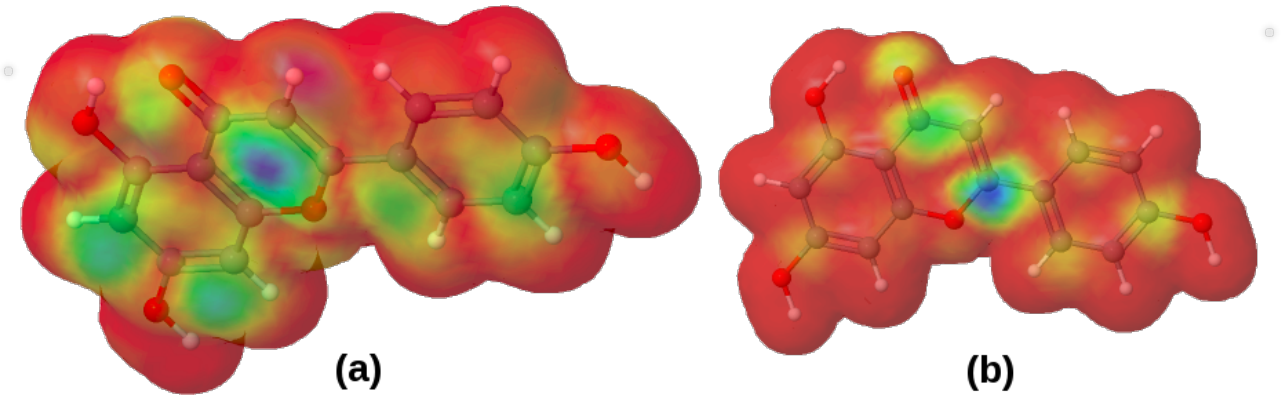

Figure 6: Apigenin electronic density maps. (a) HOMO orbital: in red, the zone most susceptible to electrophilic attacks; (b) LUMO orbital: the region most susceptible to nucleophilics attacks.

On the other hand, Table 4 shows the optimization energy values of each ligand in gaseous state, that is, before the coupling process, as well as the optimization energies after the coupling process and the energy differences for the COX-1/ligand interaction. Table 5 shows the values corresponding to COX-2/ligand interactions.

Preprints (www.preprints.org) | NOT PEER-REVIEWED | Posted: 13 February 2019 doi:10.20944/preprints201902.0124.v1

Table 4: Optimization and pos-coupling energies of COX-1/ligand complex.

COX-1						
Ligand	Luteolin	Galangin	Apigenin	Kampferol	Morin	Quercetin
Optimization Energy	-3749.02	-3452.95	-3453.72	-3748.74	-4043.90	-4044.03
MOPAC Energy	-3746.46	-3452.89	-3307.05	-3745.36	-4042.01	-4043.43
Energy Difference	-2.56	-0.05	-146.67	-3.38	-1.89	-0.60

Table 5: Optimization and pos-coupling energy values of COX-2/ligand complex

COX-2						
Ligand	Luteolin	Galangin	Apigenin	Kaempferol	Morin	Quercetin
Optimization Energy	-3749.02	-3452.95	-3453.72	-3748.74	-4043.90	-4044.03
MOPAC Energy	-3746.82	-3452.80	-3449.55	-3745.36	-4041.95	-4042.41
Energy Difference	-2.20	-0.15	-4.18	-3.38	-1.95	-1.63

Molecular Docking

For each protein-ligand complex, we selected ten different conformations and for each one we evaluated the binding energy of the complex formed. Table 6 shows the interaction energy for each conformation of Galangin/COX-1 system, the amino acids and hydrogen bonds involved. In all conformations there is formation of at least one hydrogen bonds, except the conformation 9 where there is formation of 3 hydrogen bonds. The conformation number nine have the lowest energetic values, which means that in this conformation the ligand have more stability in the active site of enzyme that others conformations.

Preprints (www.preprints.org) | NOT PEER-REVIEWED | Posted: 13 February 2019 doi:10.20944/preprints201902.0124.v1

Table 6: COX-1/Galangin complex. 1-10: ten conformations obtained with each one of the energetic values X: amino acids that interact with the ligand in each conformation. From the line upwards: presence of hydrogen bonds. Highlighted in green: amino acids that interact with the ligand and that are repeated in the indicated conformations.

Amino acids	Conformations									
	1	2	3	4	5	6	7	8	9	10
TYR 355	X	X	X	X	X	X	X	X	X	X
SER 530	X	X	X	X	X	X	X	X	X	X
ILE 523	X	X	X	X	X	X	X	X	X	X
MET 522	X	X	X	X	X	X	X	X	X	X
LEU 531	X	X	X	X	X	X	X	X	X	X
VAL 349	X	X	X	X	X	X	X	X	X	X
ALA 527	X	X	X	X	X	X	X	X	X	X
TRP 387	X		X	X	X	X	X	X	X	X
SER 353	X	X	X	X	X	X	X	X		X
LEU 352	X	X	X	X	X	X	X	X		X
TYR 385	X		X	X	X	X	X	X		X
PHE 518		X		X	X	X	X	X	X	X
GLY 526		X							X	
TYR 348	X		X							
PHE 381		X								
ARG 120									X	
VAL 116		X								
LEU 359		X								
LEU 384									X	
Bind energy	-6.96	-6.96	-6.97	-7.2	-7.18	-7.19	-7.18	-7.18	-7.26	-7.18

Most stable configuration

The selection criteria of the most stable configuration for each protein-ligand coupling, was based on energetic values, that is, the lowest interaction energy indicate the highest stability of the complex.

For each of the 6 protein-ligands pairs, the best conformation based on the aforementioned energy terms was selected. The binding energy values between all the ligands were compared in order to determine which of them best matches the active site of the protein. Table 7 shows the best conformation

Preprints (www.preprints.org) | NOT PEER-REVIEWED | Posted: 13 February 2019 doi:10.20944/preprints201902.0124.v1

for each COX-1/ligand pair and the amino acids that interact with the ligand in each conformation. The interaction is remarkable by hydrogen bonds, attraction forces, electrostatic interactions and Van der Waals dispersion forces. Table 8 shows this information for COX-2/ligand system.

Table 7: Best conformation of COX-1/ligand complex

COX-1						
Ligand	Apigenin	Kaempferol	Luteolin	Morin	Galangin	Quercetin
Conformations	1-10	1	5	6	9	3
Binding energy	-8.88	-8.24	-7.79	-7.71	-7.26	-6.65
Amino acids	TRP 387	TRP 387	TRP 387	TRP 387	TRP 387	TRP 387
	VAL 349	HIS 388	VAL 349	LEU 390	VAL 349	VAL 349
	SER 530	HIS 386	SER 530	PHE 210	SER 530	SER 530
	ILE 523	LEU 390	ILE 523	ALA 202	ILE 523	ILE 523
	GLY 526	MET 391	LEU 384	GLN 203	GLY 526	TYR 355
	ALA 527	TYR 385	TYR 385	HIS 207	MET 522	SER 353
	LEU 384	ASN 382	MET 522	ASN 382	ALA 527	TYR 385
	LEU 531	ALA 202	ALA 527	TYR 385	LEU 531	LEU 352
	MET 522	THR 206	ARG 120	THR 206	PHE 518	VAL 116
	LEU 352	HIS 207	VAL 116	HIS 388	ARG 120	TYR 348
	ARG 120	PHE 210	PHE 381	HIS 386	LEU 384	ARG 120
	TYR 355		PHE 518		TYR 355	MET 522
	VAL 116		LEU352			ALA527

Apigenin shows the lowest coupling energy in complex with COX-1, which means that this ligand have an advantage in energetic terms that others. Apigenin interact with the same amino acids in all conformations of the COX-1/Apigenin system and have the same energetic values. The ligands that follows Apigenin in terms of high energetic stability are: Kaempferol, Luteolin, Morin, Galangin and Quercetin, repectively.

Preprints (www.preprints.org) | NOT PEER-REVIEWED | Posted: 13 February 2019 doi:10.20944/preprints201902.0124.v1

Table 8: Best conformation of COX-2/ligand complex

COX-2						
Ligand	Apigenine	Kaempferol	Luteolin	Morin	Galangin	Quercetin
Conformations	7	3	1	1	3 and 8	1 and 9
Binding energy	-8.93	-7.51	-7.58	-7.91	-7.55	-7.76
Amino acids	SER 530	SER 353	VAL 523	HIS 90	TYR 355	TYR 355
	ALA 378	VAL 523	TYR 355	SER 353	VAL 523	VAL 5239
	ILE 377	HIS 90	SER 530	VAL 349	HIS 90	SER 530
	PHE 381	LEU 352	LEU 352	LEU 352	SER 353	TYR 385
	PHE 209	TYR 355	TYR 385	SER 530	LEU 352	LEU 352
	PHE 205	PHE 518	ALA 527	VAL 523	ALA 527	SER 353
	VAL 228	ILE 517	HIS 90	TYR 355	PHE 518	GLN 192
	LEU 534	GLN 192	ARG 513	MET 522	ALA 516	HIS 90
	GLY 533	ALA 516	TYR 348	LEU 384	ILE 517	PHE 518
	ASN 375	GLY 526	SER 353	TYR 385	GLN 192	ALA 527
	PHE 529	PHE 381		TRP387		
	LYS 532			PHE 518		
	ILE 124					

Table 8 shows that conformation 7 (Apignenin) have the lowest value of coupling energy, namely, is the most stable conformation of the ligand in the active site of enzyme in the coupling process. Galangin and Quercetin shows 2 conformations with the same amino acids and the same values of coupling energy. In this case, the ligands that follows Apigenin in high stability are: Morin, Quercetin, Luteolin, Galangin and Kaempferol, respectively. On the other hand, electrostatic terms has been the more relevants energetic terms to choose the conformations and the more stable ligands.

Figure 7 shows, highlighted in red, five zones of high electronic density of Apigenin, in which the hydroxyl groups of the molecule are found. Due to the high electronic density, the formation of electrostatic interactions is possible. The amino acids that interact with Apigenin are: SER 530, ALA 378, ILE 377, PHE 381, PHE 209, PHE 205, VAL 228, LEU 534, GLY 533, ASN 375, PHE 529,

Preprints (www.preprints.org) | NOT PEER-REVIEWED | Posted: 13 February 2019 doi:10.20944/preprints201902.0124.v1

LYS 532 and ILE 124. There is formation of a hydrogen bond between the amino group of ALA 378 and a hydroxyl group (OH-) of Apigenin, which helps to stabilize said conformation.

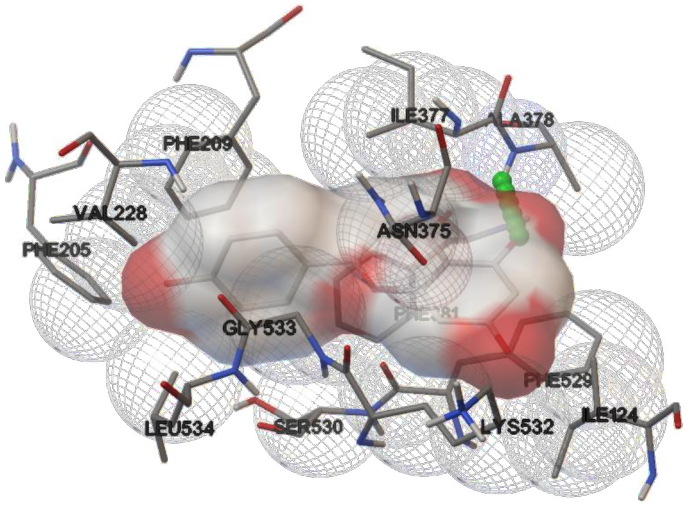

Figure 7: COX-2/Apigenin complex. The ligand is surrounded by amino acids that participate in the interaction with the active site of the enzyme. A hydrogen bond is shown in green.

Table 8 shows a comparison between the COX-1/ligand and COX-2/ligand interactions. Following the energetic terms, Apigenin have the most high stability in the active site of COX-1 with a value of -8.88 and a value of -8.93 in COX-2. While, the comparison of the coupling energy of Apigenin in COX-1 and COX-2, it shows that the stability is higher in the COX-1/Apigenin system.

Table 9: Comparison of ligand/COX-1 system and ligand/COX-2 system

Ligand	Apigenin		Galangin		Kaempferol		Luteolin		Morin		Quercetin	
Enzymes	COX-1	COX-2	COX-1	COX-2	COX-1	COX-2	COX-1	COX-2	COX-1	COX-2	COX-1	COX-2
Bind energy	-8.88	-8.93	-7.26	-7.55	-8.24	-7.51	-7.79	-7.58	-7.71	-7.91	-6.65	-7.76
Amino acids	TRP 387	SER 530	TRP 387	TYR 355	TRP 387	SER 353	TRP 387	VAL 523	TRP 387	HIS 90	TRP 387	TYR 355
	VAL 349	ALA 378	VAL 349	VAL 523	HIS 388	VAL 523	VAL 349	TYR 355	LEU 390	SER 353	VAL 349	VAL 523
	SER 530	ILE 377	SER 530	HIS 90	HIS 386	HIS 90	SER 530	SER 530	PHE 210	VAL 349	SER 530	SER 530
	ILE 523	PHE 381	ILE 523	SER 353	LEU 390	LEU 352	ILE 523	LEU 352	ALA 202	LEU 352	ILE 523	TYR 385
	GLY 526	PHE 209	GLY 526	LEU 352	MET 391	TYR 355	LEU 384	TYR 385	GLN 203	SER 530	TYR 355	LEU 352
	ALA 527	PHE 205	MET 522	ALA 527	TYR 385	PHE 518	TYR 385	ALA 527	HIS 207	VAL 523	SER 353	SER 353
	LEU 384	VAL 228	ALA 527	PHE 518	ASN 382	ILE 517	MET 522	HIS 90	ASN 382	TYR 355	TYR 385	GLN 192
	LEU 531	LEU 534	LEU 531	ALA 516	ALA 202	GLN 192	ALA 527	ARG 513	TYR 385	MET 522	LEU 352	HIS 90
	MET 522	GLY 533	PHE 518	ILE 517	THR 206	ALA 516	ARG 120	TYR 348	THR 206	LEU 384	VAL 116	PHE 518
	LEU 352	ASN 375	ARG 120	GLN 192	HIS 207	GLY 526	VAL 116	SER 353	HIS 388	TYR 385	TYR 348	ALA 527
	ARG 120	PHE 529	LEU 384		PHE 210	PHE 381	PHE 381		HIS 386	TRP 387	ARG 120	
	TYR 355	LYS 532	TYR 355				PHE 518			PHE 518	MET 522	
	VAL 116	ILE 124					LEU 352				ALA 527	

Preprints (www.preprints.org) | NOT PEER-REVIEWED | Posted: 13 February 2019 doi:10.20944/preprints201902.0124.v1

Stability Index SI

We have been established a stability index according to the energy values (bind energies) of each protein-ligand interaction. We quantified the force exerted by the interaction of the ligand with the active site of enzyme. The interaction index is defined as follows:

$$IE = \frac{E_i}{E_{minor}} \tag{1}$$

Where, E_i represent the bind energy of each protein-ligand interaction and E_{minor} is the minor bind energy of all protein-ligand interaction. The IE is normalized as follows:

$$IEN = \frac{(E_j - E_{minor})}{(E_{mayor} - E_{minor}} \tag{2}$$

Where, IEN is the normalized stability index, E_i represent the bind energy of each protein-ligand interaction, E_{minor} is the minor bind energy of all protein-ligand interaction and E_{higher} is the higher bind energy of all protein-ligand interactions.

Figure 8(a) represent the greater stability of Apigenin in the active site of COX-1, followed by Kaempferol, Luteolin, Morin, Galangin and Quercetin with the lowest stability. While, Figure 8(b) shows that Apigenin was the ligand more stable in the active site of COX-2, followed by Morin, Quercetin, Luteolin, Galangin and Kaempferol. In the region of the ligands with the lowest stability, that is, 0.51, we find Luteolin, Morin, Galangin and Quercetin.

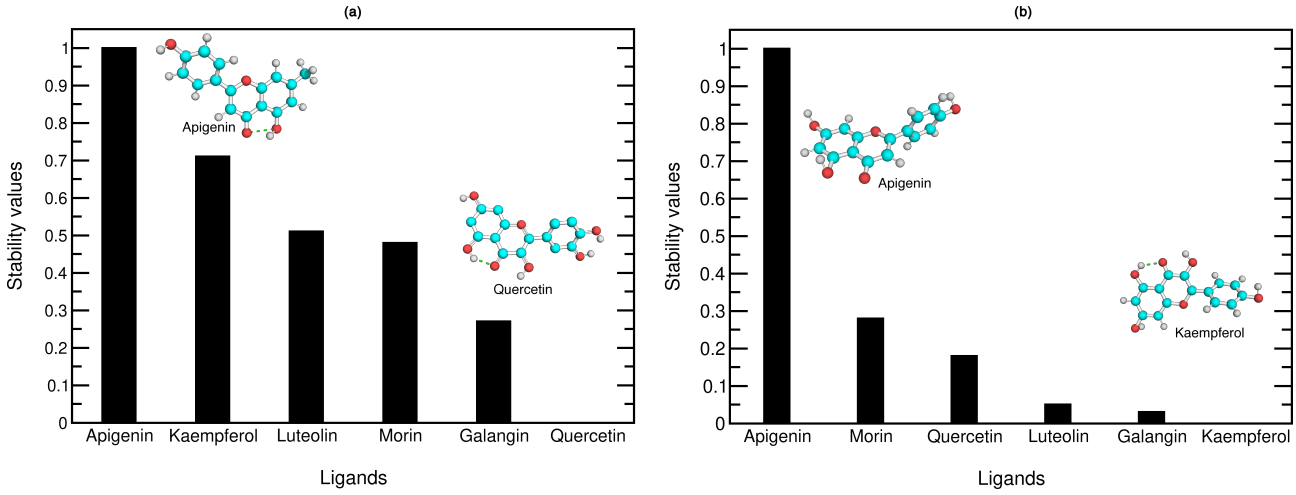

Figure 8: Selectivity index of ligands. (a) selectivity index for COX-1; (b) selectivity index for COX-2.

Quercetin have the lowest relative stability index of all ligands in complex with COX-1, while

Preprints (www.preprints.org) | NOT PEER-REVIEWED | Posted: 13 February 2019 doi:10.20944/preprints201902.0124.v1

the same ligand has a higher stability index in complex with COX-2 (IE 0.18), which means that this ligand can be the structure with more energetic differences between both active sites.

On the other hand, Kaempferol have the higher stability index in COX-1 (IE 0.71) while this index is close to zero in COX-2. This suggest that Kaempferol is in a low energy state in the active site of COX-1. Table 10 shows a comparison of the energetic parameters and the formation of interactions between the ligands with IE values more representatives.

Table 10: Energetic parameters and hydrogen bonds formation of Apigenin, Quercetin and Kaempferol.

Ligand	Apigenin		Quercetin		Kaempferol	
Enzymes	COX-1	COX-2	COX-1	COX-2	COX-1	COX-2
Heat of Formation kJ mol	-362.63	-235.67	-917.04	-813.97	-467.72	-469.34
Total Energy eV	-3307.05	-3449.55	-4043.43	-4042.41	-3745.36	-3745.36
Electronic Energy eV	-21346.54	-21448.13	-25951.83	-25836.36	-23672.59	-23641.45
Core-Core Repulsion eV	18039.48	17998.58	21908.39	21793.95	19927.22	19896.09
Ionization Potential eV	9.21	9.52	9.17	9.09	9.06	9.17
HOMO Energy eV	-9.21	-9.52	-9.17	-9.09	-9.06	-9.17
LUMO Energy eV	-1.36	-0.99	-1.21	-1.37	-1.53	-1.44

Figure 9 shows the interaction of Apigenin, Quercetin and Kamepferol with COX, also highlighted the amino acids of active sites and the hydrogen bonds formed.

Preprints (www.preprints.org) | NOT PEER-REVIEWED | Posted: 13 February 2019 doi:10.20944/preprints201902.0124.v1

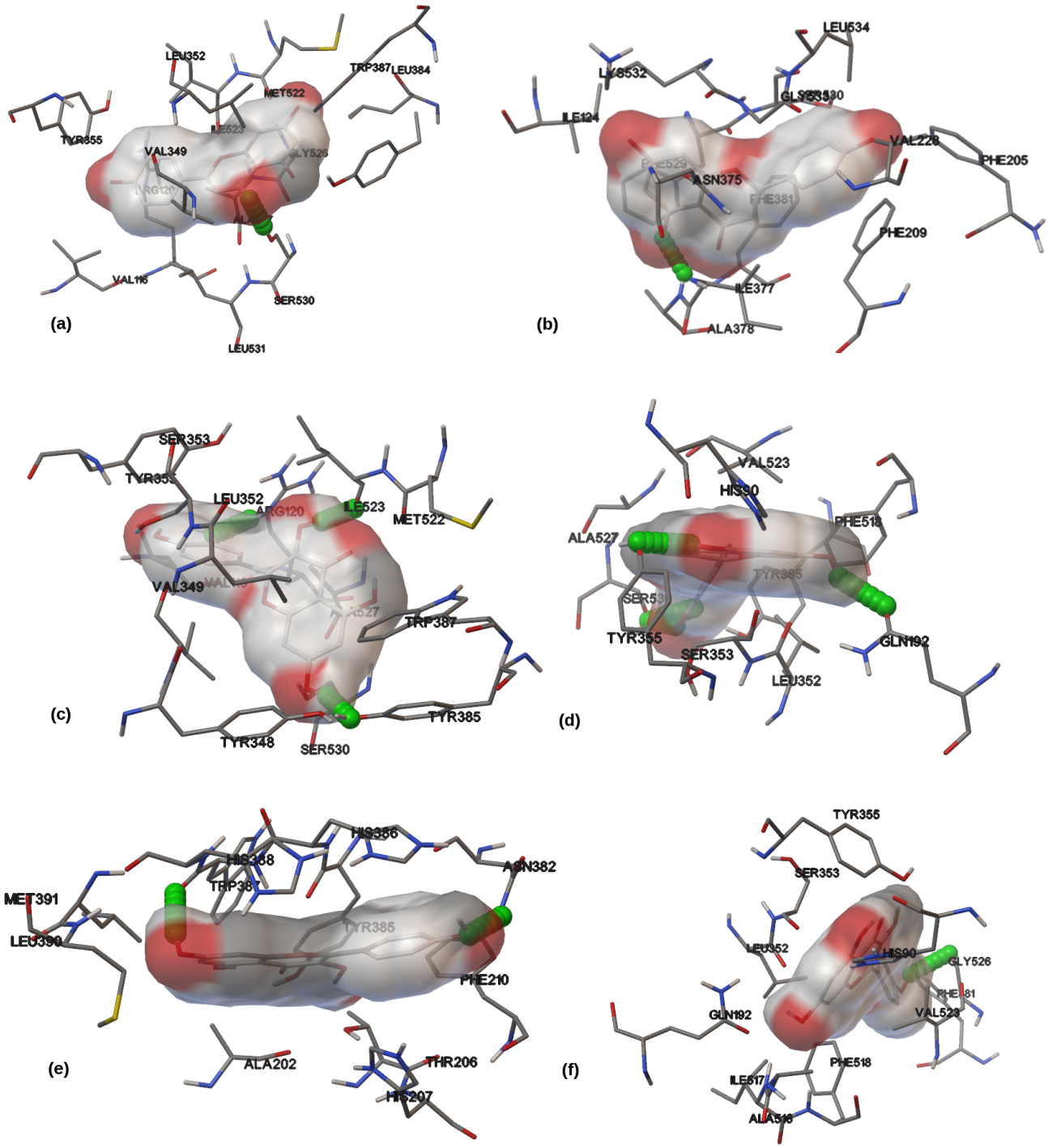

Figure 9: COX-Ligands complex. (a) COX-1/Apigenin system; (b) COX-2/Apigenin system; (c) COX-1/Quercetin system; (d) COX-2/Quercetin system; (e) COX-1/Kaempferol system; (f) COX-2/Kaempferol system. In all complexes, the ligand is surrounded by amino acids of the enzyme active site. In green the hydrogen bonds formed.

Selectivity Index of Protein Ligands SIPL

The SIPL is a very important parameter to quantify the potential that some ligands have to inactivate a enzyme. This index shows the affinity for one or another isomeric form of COX in numerical and relative form.

Preprints (www.preprints.org) | NOT PEER-REVIEWED | Posted: 13 February 2019 doi:10.20944/preprints201902.0124.v1

The ISPL is calculated by dividing the binding energy of each COX-2/ligand interaction between the binding energy of each COX-1/ligand interaction, taking into account the correspondence between the ligands.

The ISPL is defined as follows:

$$IS = \frac{\frac{E_i,COX2 - E_{min},COX2}{E_{hig},COX2 - E_{min},COX2}}{\frac{E_i,COX1 - E_{min},COX1}{E_{hig},COX1 - E_{min},COX1}} \tag{3}$$

Quercetin was the ligand with a higher SIPL in the active sites of both enzymes, followed by Galangin, Morin, Apigenin, Luteolin and Kaempferol.

Figure 10 shows the ISPL in a descent form. First, Quercetin have the higher value of selectivity with 1.17, while Kaempferol shows the lowest value with 0.91. Finally, we can notice that the difference in the ISPL values is not very marked among the ligands, which is very notable in the values of the stability index where the difference is greater.

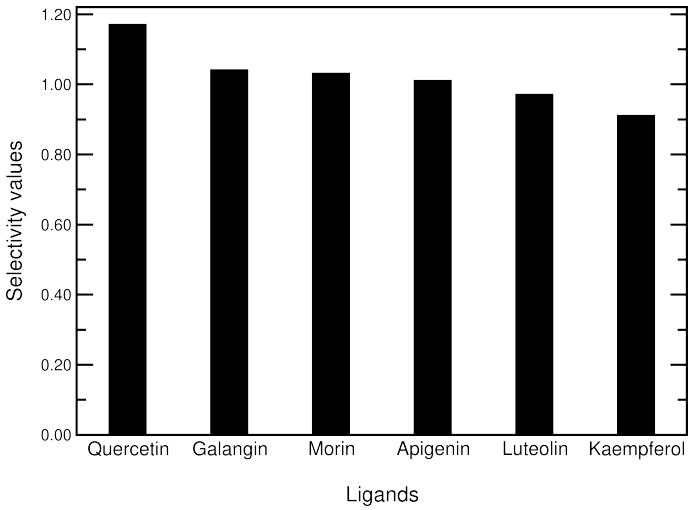

Figure 10: Selectivity index of ligands.

Conclusions

Las interacciones de los flavonoides con los aminoácidos del sitio activo de las enzimas se dan principalmente a través de los grupos hidroxilos que presentan en su estructura. El número de dichos grupos -OH varían de acuerdo al tipo de flavonoide, pero es importante notar que un metabolito por tener más grupos -OH que otro no lo hace más estable o selectivo.

• Los Puentes de Hidrógeno, aunque son un tipo de interacción muy importante, no definen la estabilidad de los ligandos durante el el acople, es decir que el hecho que un metabolito forme mayor

 doi:10.20944/preprints201902.0124.v1

número de enlaces de hidrógenos que otro no garantiza que siempre será el más estable.

• Con base a lo anterior, es de resaltar que tanto la estabilidad como la selectividad de los ligandos son parámetros independientes, es decir, que el hecho que un ligando sea estable en el sitio activo de la enzima no quiere decir que también sea muy selectivo por la misma; esto se puede ver al comparar las gráficas de estabilidad y selectividad donde para el primer caso, la apigenina presentó un mayor índice de estabilidad que el resto de los ligandos, lo cual no sucedió en el índice de selectividad.

Supplementary Information SI

Acknowledgments

References

1. Combariza, A. F.; Sullivan, E.; Auerbach, S. M.; Blanco, C. ; *J. Phys. Chem. B.* **2005**, *109*, 18439.
2. Combariza, A. F.; Gomez, D. A.; Sastre, G. ; *Chem. Soc. Rev. 2013*, **42**, 114.
3. Marti, S.; Moliner, V.; Andres, J.; Roca, M.; Lopez-canut, V.; Silla, E.; Tunon, I.; Bertran, J.; *An. Quim.* **2011**, *107*, 144.
4. Combariza, A. F.; Sastre, G.; *J. Phys. Chem. C.* **2011**, *115*, 13751.
5. Lippow, S. M.; Tidor, B.; *Curr. Opin. Biotechnol.* **2007**, *18*, 305.
6. Paquet, E.; Viktor, H. L.; *Biomed Res. Int.* **2015**, *2015*, 1.
7. Ferreira, L. G.; Dos Santos, R. N.; Oliva, G.; Andricopulo, A. D. ; *Molecules.* **2015**, *20*, 13384.
8. Levine, I.; Rodriguez, A.; Pascual, A.; Roman, J.; *Quantum Chemistry*, 6th ed.; Pearson Education: New York, USA, 2009.
9. Perez, J. D.; *J. Trop. Eng.* **2014**, *24*, 117.
10. Kitchen, D. B.; Decornez, H.; Furr, J. R.; Bajorath, J.; *Nat. Rev. Drug Discov.* **2004**, *3*, 935.
11. Fitzpatrick, F. A.; *Curr. Pharm. Des.* **2004**, *10*, 577.

12. Rouzer, C. A.; Marnett, L. J.; *J. Lipid Res.* **2009**, *50 Suppl*, S29.

13. Limongelli, V.; Bonomi, M.; Marinelli, L.; Gervasio, F. L.; Cavalli, A.; Novellino,, E.; Parrinello, M.; *Proc. Natl. Acad. Sci. U. S. A.* **2010**, *107*, 5411.

14. Garavito, R. M.; DeWitt, D. L.; *Biochim. Biophys. Acta.* **1999**, *1441*, 278.

15. Mohammed, M. S.; Osman, A. J.; Garelnabi, E. A.; Osman, Z.; Osman, B.; Khalid, H. S.; Mohamed, M. A.; Osman, J. A. *J. Phytopharm.* **2014**, *3*, 275.

16. Aswad, M.; Rayan, M.; Abu-Lafi, S.; Falah, M.; Raiyn, J.; Abdallah, Z.; Rayan, A.; *Inflamm. Res.* **2018**, *67*, 67.

17. Kumar, S.; Pandey, A. K.; Kumar, S.; Pandey, A. K. ; *Sci. World J.* **2013**, *2013*, 1.

18. Chen, H. J.; Chung, C. P.; Chiang, W.; Lin, Y. L.; *Food Chem.* **2011**, *126*, 1741.

19. `https://www.rcsb.org/`, accesed in June 2018.

20. Wishart, D. S.; Feunang, Y. D.; Guo, A. C.; Lo, E. J.; Marcu, A.; Grant, J. R.; Sajed, T.; Johnson, D.; Li, C.; Sayeeda, Z.; Assempour, N.; Iynkkaran, I.; Liu, Y.; Maciejewski, A.; Gale, N.; Wilson, A.; Chin, L.; Cummings, R.; Le, D.; Pon, A.; Knox, C.; Wilson, M.; *Nucleic Acids Res.* **2018**, *46*, D1074.

21. Sidhu, R. S.; Lee, J. Y.; Yuan, C.; Smith, W. L.; *Biochemistry.* **2010**, *49*, 7069.

22. Picot, D.; Loll, P. J.; Garavito, R. M.; *Nature.* **1994**, *367*, 243.

23. Kurumbail, R. G.; Stevens, A. M.; Gierse, J. K.; McDonald, J. J.; Stegeman, R. A.; Pak, J. Y.; Gildehaus, D.; Iyashiro, J. M.; Penning, T. D.; Seibert, K.; Isakson, P. C.; Stallings, W. C. *Nature.* **1996**, *384*, 644.

24. Drenth, J.; Mesters, J.; *Principles of protein X-ray crystallography*, 3th ed.; Springer New York: New York, USA, 2007.

25. Humphrey, W.; Dalke, A.; Schulten, K.; *J. Mol. Graph.* **1996**, *14*, 33.

26. Yuan, S.; Chan, S. H.; Hu, Z.; *Wiley Interdiscip. Rev. Comput. Mol. Sci.* **2017**, *7*, e1298.

27. `http://www.chemspider.com/`, accessed in June 2017.

28. Pence, H. E.; Williams, A.; *J. Chem. Educ.* **2010**, *87*, 1123.

29. www.chemspider.com/Chemical-Structure.4444100.html, accessed in June 2018.

30. www.chemspider.com/Chemical-Structure.4444102.html, accessed in June 2018.

31. Feng, B. Y.; Toyama, B. H.; Wille, H.; Colby, D. W.; Collins, S. R.; May, B. C.; Prusiner, S. B.; Weissman, J.; Shoichet, B. K.; *Nat. Chem. Biol.* **2008**, *4*, 197.

32. www.chemspider.com/Chemical-Structure.4444989.html, accessed in June 2018.

33. www.chemspider.com/Chemical-Structure.4444935.html, accessed in June 2018.

34. www.chemspider.com/Chemical-Structure.4444395.html, accessed in June 2018.

35. Cuevas, G.; Cortes, F.; *Introduccion a la quimica computacional*, 1ra ed.; Fondo de Cultura Economica: Mexico, 2003.

36. Foresman, J. B.; Frisch, Ae.; *Exploring Chemistry With Electronic Structure Methods*, 3th ed.; Gaussian, Inc.: Wallingford, CT, 2015.

37. Schlegel, H. B.; *Wiley Interdiscip. Rev. Comput. Mol. Sci.* **2011**, *1*, 790.

38. Zheng, J.; Frisch, M. J.;
newblock *J. Chem. Theory Comput.* **2017**, *13*, 6424.

39. Schlegel, H. B.; *J. Comput. Chem.* **2003**, *24*, 1514.

40. http://openmopac.net/, accessed in July 2018.

41. Stewart, J. J.; *J. Comput. Aided. Mol. Des.* **1990**, *4*, 1.

42. Boyd, D. B.; Smith, D. W.; Stewart, J. J. P.; Wimmer, E.; *J. Comput. Chem.* **1988**, *9*, 387.

43. Stewart, J. J.; *J. Mol. Model.* **2004**, *10*, 155.

44. Dewar, M. J.; Thiel, W.; *J. Am. Chem. Soc.* **1977**, *99*, 4899.

45. http://vina.scripps.edu/, accessed in July, 2018).

46. Trott, O.; Olson, A. J.; *J. Comput. Chem.* **2009**, *31*, NA.

 doi:10.20944/preprints201902.0124.v1

47. Morris, G. M.; Goodsell, D. S.; Halliday, R. S.; Huey, R.; Hart, W. E.; Belew, R. K.; Olson, A. J.; *J. Comput. Chem.* **1998**, *19*, 1639.

48. Fuhrmann, J.; Rurainski, A.; Lenhof, H.-P.; Neumann, D.; *J. Comput. Chem.* **2010**, *31*, NA.

49. DeWitt, D. L.; El-Harith, E. A.; Kraemer, S. A.; Andrews, M. J.; Yao, E. F.; Armstrong, R. L.; Smith, W. L. ; *J. Biol. Chem.* **1990**, *265*, 5192.

50. Lecomte, M.; Laneuville, O.; Ji, C.; DeWitt, D. L.; Smith, W. L.; *J. Biol. Chem.* **1994**, *269*, 13207.

51. Mancini, J. A.; Riendeau, D.; Falgueyret, J. P.; Vickers, P. J.; O'Neill, G. P.; *J. Biol. Chem.* **1995**, *270*, 29372.

52. Rieke, C. J.; Mulichak, A. M.; Garavito, R. M.; Smith, W. L.; *J. Biol. Chem.* **1999**, *274*, 17109.

53. Zarghi, A.; Arfaei, S. *Iran. J. Pharm. Res.* **2011**, *10*, 655.